ResearchGate

See discussions, stats, and author profiles for this publication at: https://www.researchgate.net/publication/26821776

Determination of the Aerosol Yield of Isoprene in the Presence of an Organic Seed with Carbon Isotope Analysis

ARTICLE *in* ENVIRONMENTAL SCIENCE AND TECHNOLOGY · SEPTEMBER 2009

Impact Factor: 5.33 · DOI: 10.1021/es9006959 · Source: PubMed

CITATIONS
16

READS
28

9 AUTHORS, INCLUDING:

Josef Dommen
Paul Scherrer Institut
172 PUBLICATIONS **6,052** CITATIONS
SEE PROFILE

Maya Jäggi
Paul Scherrer Institut
34 PUBLICATIONS **527** CITATIONS
SEE PROFILE

Rolf Theodor Walter Siegwolf
Paul Scherrer Institut
238 PUBLICATIONS **5,554** CITATIONS
SEE PROFILE

Martin Fierz
University of Applied Sciences and Arts Nor…
47 PUBLICATIONS **493** CITATIONS
SEE PROFILE

All in-text references underlined in blue are linked to publications on ResearchGate, letting you access and read them immediately.

Available from: Rolf Theodor Walter Siegwolf
Retrieved on: 03 February 2016

Determination of the Aerosol Yield of Isoprene in the Presence of an Organic Seed with Carbon Isotope Analysis

JOSEF DOMMEN,*,† HEIDI HELLÉN,†,§ MATTHIAS SAURER,† MAYA JAEGGI,†,∥ ROLF SIEGWOLF,† AXEL METZGER,†,⊥ JONATHAN DUPLISSY,† MARTIN FIERZ,‡ AND URS BALTENSPERGER†

Laboratory of Atmospheric Chemistry, Paul Scherrer Institut, 5232 Villigen PSI, Switzerland, and Fachhochschule Nordwestschweiz, 5210 Windisch, Switzerland

Received March 5, 2009. Revised manuscript received June 15, 2009. Accepted June 29, 2009.

We examined a new method to determine the aerosol yield of precursors of secondary organic aerosols in the presence of organic seed particles. To distinguish between the oxidation products of the compound in question and the organic seed, the compound was labeled with stable isotopes and aerosol samples were analyzed by isotope ratio mass spectrometry (IRMS). ^{13}C labeled isoprene was obtained from isoprene emitting plants that were exposed to $^{13}CO_2$. The aerosol yield of isoprene was determined from the $^{13}C/^{12}C$ ratio measured in the aerosol. Measurements at organic aerosol mass concentrations as low as 10 μg m^{-3} were performed. Three different methods of aerosol sampling procedures were evaluated: impactor, filter, and electrostatic deposition. The excess-% ^{13}C measured by the three sampling methods agreed well. The aerosol yield of isoprene derived from these measurements showed a strong dependence on further oxidation of first-generation products and is within the range of reported yield values (1−5%) obtained so far from pure isoprene experiments.

Introduction

Secondary organic aerosol (SOA) is particulate matter that is formed by gas-to-particle conversion of the oxidation products of volatile organic compounds (VOCs). SOA constitutes a substantial fraction of the organic mass of atmospheric aerosols (*1*). Recent field studies indicate that SOA is significantly more abundant in various regions of the troposphere than state-of-the-art SOA models predict (*2*). These estimates are based on laboratory data from oxidation experiments of individual precursors leading to SOA formation. The current state of knowledge on the global SOA budget is summarized in Hallquist et al. (*3*). They conclude from a comparison between bottom-up model estimates and various top-down approaches that the global SOA budget is at present still poorly constrained.

* Corresponding author e-mail: josef.dommen@psi.ch; tel: +41 56 310 2992; fax: +41 56 310 4525.
† Paul Scherrer Institut.
‡ Fachhochschule Nordwestschweiz.
§ Now at Finnish Meteorological Institute, Helsinki, Finland.
∥ Now at Department Logistics for Radiation Safety and Security, Radioanalytics, Paul Scherrer Institut, 5232 Villigen PSI, Switzerland.
⊥ Now at Ionicon Analytik Gesellschaft M.B.H., Innsbruck, Austria.

The aerosol yield (Y) is equal to the mass of SOA produced (ΔM_{OA}) divided by the mass of a precursor hydrocarbon (ΔM_{HC}) that has reacted. Several factors complicate the determination of aerosol yields from smog chamber studies: (1) During the course of the experiment aerosols are lost to the chamber walls. This may also happen with semivolatile species, which reduces their partitioning into the aerosol. These losses complicate the mass balance (*4*). Under ambient conditions there is always an inorganic/organic aerosol available onto which oxidation products can condense, whereas in laboratory studies the organic particle phase is usually only formed in the process of SOA formation. If SOA is only formed after a longer induction period, semivolatile first-generation products are subject to increased wall losses and ongoing chemical degradation (*5*). Thus yields measured in chambers may be substantially lower than those under ambient conditions. (2) There is always an equilibrium of the species between the gas and particle phase which depends on the existing particle mass and on its composition. However, experiments in chambers are usually performed with one SOA precursor and thus the composition of the SOA can not be varied. (3) Chemical reactions such as oligomerization may occur in the condensed phase (*6*). The extent and type of these reactions may depend on the composition of the aerosol and thus influence the aerosol yield of a precursor gas. (4) Smog chamber experiments are often performed at higher than ambient concentrations, and the extrapolation to lower concentrations is not trivial.

In this work we show how the SOA yield of a specific precursor can be determined in the presence of an organic seed particle. Such a measurement technique would then allow determining SOA yields of compounds as a function of the composition of the organic aerosol. To study the SOA formation potential of a specific organic precursor in the presence of an organic aerosol requires differentiating the organic seed aerosol compounds from the partitioned oxidation products of this precursor. This can be achieved by isotopic labeling of either the precursor or the compounds of the organic seed. Offenberg et al. (*7*) used ^{14}C as a tracer to distinguish between the contribution of toluene (fossil carbon without ^{14}C) and α-pinene (modern carbon with the contemporary content of ^{14}C) to SOA in a mixture. Since the abundance of ^{14}C is very low these experiments had to be performed at high precursor concentrations (hundreds of ppb) which are not representative for ambient conditions. In this study we examine the labeling of compounds with stable isotopes and the use of isotope ratio mass spectrometry (IRMS) to measure the SOA formation potential of compounds in the presence of organic seed aerosols. This method is demonstrated by investigating the SOA yield of ^{13}C labeled isoprene at precursor mixing ratios of 10−20 ppb and organic particle concentrations of 10−30 μg m^{-3} which are atmospherically relevant.

Isoprene (2-methyl-1,3-butadiene, C_5H_8) was chosen because its global emission has been estimated at ∼500 Tg yr^{-1}, which is far higher than those of biogenic terpenes and anthropogenic hydrocarbons (*8*). The impact of such a potentially large source of carbonaceous aerosol necessitates careful investigation of the fate of isoprene oxidation products on a global scale. Recent laboratory chamber studies of isoprene photooxidation showed SOA formation at precursor concentrations as low as 10 ppb (*9*−*11*). At an aerosol concentration of 5 μg m^{-3} Dommen et al. (*11*) obtained SOA mass yields of 0.006 for isoprene to NO_x ratios of 2. Kroll et al. (*9, 10*) reported SOA mass yields of 0.015 under high NO_x conditions and even 0.029 in the absence of NO_x. This

10.1021/es9006959 CCC: $40.75 © 2009 American Chemical Society
Published on Web 07/29/2009

presents a factor of 5 difference in aerosol yield between the lowest and highest number, which becomes even larger at lower aerosol mass concentrations (see refs *10, 11)*. The pronounced scatter of SOA yields measured in these studies is most probably due to different experimental conditions like VOC to NO_x ratios, different OH radical precursors used, leading to different OH levels and the point of the reaction sequence where the yield was determined. Isoprene has two double bonds which are easily oxidized in consecutive reactions. The main first-generation oxidation products of isoprene are formaldehyde, methacrolein, and methylvinylketone. Ng et al. (*26*) have shown that SOA formation strongly depends on further oxidation of methacrolein.

Depending on the yields used from laboratory experiments model studies calculated a small or large contribution of isoprene to atmospheric particulate organic matter (OM) (*12*−*15*). Based on the aerosol yields of the no-NO_x experiments of Kroll et al. (*10*), Henze and Seinfeld (*12*) calculated an increase of the global burden of SOA by a factor of 2 when isoprene was included as a source of SOA. Similarly, isoprene SOA was predicted to increase the total OM by up to 56% in the planetary boundary layer and 90% in the free troposphere (*14*). This illustrates the large potential of isoprene SOA formation and the need to reduce uncertainties in the yield.

Experimental Section

^{13}C Labeled Isoprene Generation. $^{13}C/^{12}C$ ratios in hydrocarbons are typically in the range of 0.0112 and variations as little as 0.000006 can be quantified by IRMS. To differentiate isoprene products from the organic seed aerosol compounds one needs to label all five carbons of isoprene by ^{13}C. To produce this ^{13}C labeled isoprene we exploited the capability of plants to quickly produce and emit isoprene as a byproduct of photosynthetic CO_2 fixation (*16*). Six potted velvet bean plants (*Mucuna pruriens)* were placed in a 184-L Plexiglas chamber to produce ^{13}C labeled isoprene. The chamber was flushed with pure CO_2-free air to reduce the CO_2 concentration in the plant chamber as much as possible (ca. 50 ppm). As soon as this low CO_2 level was reached, highly enriched $^{13}CO_2$ (carbon dioxide, 99% ^{13}C, Cambridge Isotope Laboratories, Inc.) was added until 600−700 ppm CO_2 was reached. The photosynthetically active photon flux density was set to 900 μmol m^{-2} s^{-1} using two 400-W lamps (Powerstar HQI-T, Osram, Germany) on top and a 500-W lamp (Philips Plus Y9A) on two opposite sides of the chamber each. Two xenon lamps on top and one on two opposite sides of the chamber were turned on to initiate the photosynthesis. The isoprene production started simultaneously with the photosynthetic CO_2 assimilation and increased to a constant maximal level. The CO_2 level was kept constant by replenishing the assimilated $^{13}CO_2$. The roots and soil of the plants were enclosed in plastic bags to minimize the $^{13}CO_2$ emissions from soil respiration. To follow contamination of the air with $^{13}CO_2$ we monitored both $^{12}CO_2$ and $^{13}CO_2$ concentrations with two infrared gas analyzers (IRGA, Li-7000 LI-COR, Nebraska for $^{12}CO_2$ only and a Binos II, Leybold Haereus, Vötsch, Germany for $^{12}CO_2$ + $^{13}CO_2$). The selective IR-filter in the Binos II instrument was removed to measure both isotopologues. A water trap, set to a constant temperature of 2 °C, reduced the interference of water vapor for both instruments. The temperature in the chamber was kept below 35 °C by ventilators. As the isoprene emission decreased after 5 days the plants were replaced, which also helped to avoid additional stress-induced emissions of impurities produced by the plants during the experiments. The isoprene concentration and its degree of labeling were checked regularly by proton transfer reaction mass spectrometry (PTR-MS) (Ionicon). As shown in Figure 1, 70−80% of carbon was already labeled after 1 h, and on average a final labeling of 81 ± 2% was obtained.

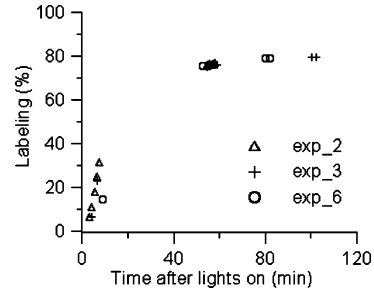

FIGURE 1. Time development of the ^{13}C labeling in isoprene emitted from plants in three different experiments as measured by PTR-MS.

TABLE 1. Initial Concentrations of α-Pinene and Isoprene, Maximum SOA Mass (μg m^{-3}) Measured by SMPS

experiment	isoprene (ppb)	α-pinene (ppb)	SOA (max) (μg m^{-3})[a]
1	16.7	30	41.5
2	19.8	30	48.1
3	10.6	30	29.4
4	11.5	12	12.5
5	21.6	30	30.9
6	12.7	120	191

[a] Wall-loss-corrected SOA mass concentrations assuming a density of 1.3 g cm^{-3}.

Smog Chamber Experiments. When the isoprene level in the plant chamber reached a sufficient concentration (∼2200−4100 ppb) the air−isoprene mixture was flushed with pure air through two cold traps (−131 °C) to remove water vapor and impurities (e.g., monoterpenes emitted by the plants) to the large smog chamber. The remaining impurities in the transferred air were measured after the trap by PTR-MS and were found to be negligibly small (<0.1%). The photooxidation experiments were performed at 20 °C and 50% relative humidity in the PSI 27-m^3 smog chamber described in detail by Paulsen et al. (*17*). Various amounts of α-pinene (98%, Aldrich) were added (see Table 1) followed by nitrous acid (HONO), which was continuously injected into the smog chamber as an OH radical source. Thereafter photooxidation of the mixture was started by turning on four xenon-arc lamps.

HONO was produced in situ in a flow-type generation system based on the reaction of sodium nitrite solution with sulfuric acid (*18*). The HONO flow was kept low to ensure that the NO concentration was below 0.5 ppb ensuring a low NO_x-chemistry. Thus, in our experiments both NO + HO_2/RO_2 and HO_2 + RO_2 reactions always occurred simultaneously. Contrary to "standard" experiments with NO_x there was no transition from solely NO + HO_2/RO_2 reactions to predominantly HO_2 + RO_2 reactions.

A scanning mobility particle sizer (SMPS, consisting of a differential mobility analyzer (DMA, TSI 3071) and a condensation particle counter (CPC, TSI 3022)) measured the particle size distribution, which was converted to a mass concentration assuming spherical particle geometry with a density of 1.3 g cm^{-3} (*19, 20*). The aerosol mass concentration was corrected for wall-loss fitting the measured change of the aerosol size distribution. The PTR-MS instrument was used for the measurement of isoprene, α-pinene, and the sum of methacrolein and methylvinylketone (MACR + MVK), which have the same molecular weight. It was calibrated using gas standards (Apel-Riemer Environmental Inc., Denver, CO). O_3, NO, and NO_2 were all continually monitored (*17*).

SOA was sampled by three methods for ^{13}C analysis. First, SOA was sampled on quartz fiber filters behind charcoal

denuders (Novacarb monolith synthetic carbon, Mastcarbon Ltd., Guilford, UK) to strip off the gas phase. This type of sampling may suffer from positive artifacts from adsorbing gaseous species (if denuders are not 100% efficient) or negative artifacts by evaporation of semivolatile species. Second, aerosols were positively charged in a unipolar diffusion charger and deposited on tin foils held at a high negative potential (−5 kV) in an electrostatic deposition chamber (similar to Fierz et al., (*21*)). In this method there is minimal influence of gaseous species and all particles are collected on one substrate. The deposition chamber was designed to collect the aerosol with close to 100% efficiency, which was checked by comparing the IRMS data with volume concentrations derived from SMPS size distribution measurements and was found to be 25%. This number is substantially lower than the theoretical value, the reason for which is currently not known. Third, samples were collected on tin foils on the last 6 stages of an 11-stage impactor (*22*). This method results in minimal influence of gaseous species but the sample is distributed among different stages affecting the limit of detection. At low pressures a part of the more volatile particle fraction could also evaporate. The collection efficiency of the impactor was less than 30% as measured by IRMS and SMPS. The flow rates for the impactor and electrostatic sampler were 9.8 and 1.5 L/min, respectively, and for the filters was 1.8−3.9 L/min. The sampling times varied between 90 and 180 min. During an experiment 1−3 sets of samples were taken.

Isotope Ratio Analysis. Immediately after particle sampling the different samples were burnt in oxygen in an elemental analyzer (EA-1110, Carlo Erba Thermoquest, Milan, Italy) coupled in continuous-flow mode to the inlet of the isotope ratio mass spectrometer (Delta S, Thermo Finnigan, Bremen, Germany) and the $^{13}C/^{12}C$ ratio of CO_2 was measured as relative deviations from the international standard ($\delta^{13}C$ values), which is Vienna Peedee Belemnite (VPDB) for carbon. From these values, we calculated the fraction f of ^{13}C ($^{13}C/(^{13}C + ^{12}C)$) (*23*). The mass-spectrometer signal of CO_2 was also used for C-amount determination, where the combustion of standards with known C-contents provided a relationship between the CO_2 peak area in the IRMS and the C-amount in μg C. The isotope analysis of organic samples in the μg range as required in this study is challenging due to the carbon blank, which originates from the tin or silver foils that were used during the analysis. Ultralight weight tin foils (D1073, Elemental Microanalysis, Devon, UK)) were found to have the lowest blank. A surface cleaning procedure (acetone, DI water, heating at 120 °C) resulted in a further 30% reduction of the blank. We obtained a minimal blank of 0.23 μg C per cm^2 foil. Quartz filters preheated at 800 °C were not carbon free either: 6 mm diameter punched discs used during the experiments contained 0.59 μg ± 0.04 μg C. The ^{13}C fraction of the blank and α-pinene was measured to be 0.010838 (equivalent to $\delta^{13}C = -25$‰) and 0.010805 ($\delta^{13}C = -27.9$‰) respectively.

Results and Discussion

Since the photooxidation of α-pinene produces SOA much faster than the one of isoprene, α-pinene SOA serves as organic seed for the isoprene oxidation products. The amount of organic seed was varied by the addition of different amounts of α-pinene. The values of the initial concentrations of α-pinene, isoprene, and the maximum SOA mass concentrations are presented in Table 1. Figure 2 shows the time profiles of some gas phase species as well as of the aerosol mass from experiment 2. Isoprene and α-pinene were entirely consumed within 8 h. The temporal evolution of the mixing ratio of isoprene could not be measured directly since the mass-to-charge signals of the different isotopologues overlap with the mass-to-charge signals of the isotope labeled

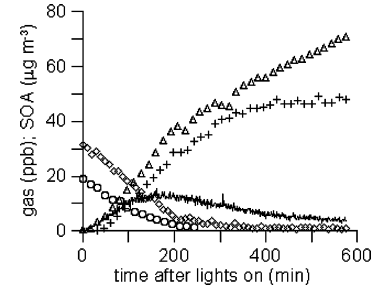

FIGURE 2. Time profiles of the gas phase species (ppb) isoprene (○), α-pinene (◊), O_3 (Δ), methylvinylketone + methacrolein (line), and SOA (+) mass concentration (μg m^{-3}) in experiment 2.

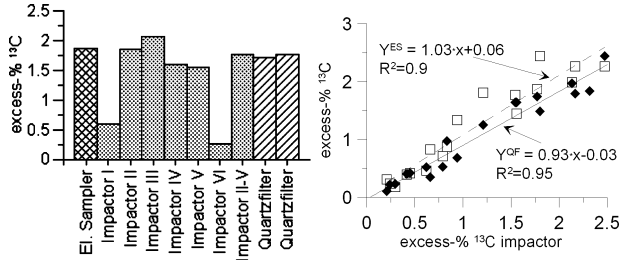

FIGURE 3. (a) Excess-% ^{13}C in all samples of experiment 5. (b) Excess-% ^{13}C of isoprene measured from the electrostatic sampler (□) and quartz filters (average) (◆) plotted versus results of impactor (average of stages II−V).

methylvinylketone and methacrolein. Unlabeled, both of these compounds have a molecular weight of 70. Therefore isoprene concentrations were determined by calculating its consumption from its reaction with ozone and OH. Ozone was measured during the experiment and OH radicals were calculated from the decay of α-pinene taking into account its reaction with O_3. Methylvinylketone + methacrolein concentrations were determined from the m/z 75 signal which belongs to the fully labeled compound assuming that only the fully labeled MVK + MACR contributes to this signal. Methylvinylketone + methacrolein concentrations increase during 180 min after lights were switched on and then start to slowly decrease due to reactions with OH radicals and photolysis. Ozone steadily increases but its contribution to the isoprene and α-pinene decay is small. Particles appear after 30 min and the maximum SOA mass concentration is reached after 7 h.

Comparison of Sampling Methods. Aerosol samples were collected at different times of the experiment by the three different methods. Figure 3a shows the excess-% ^{13}C originating from isoprene in the first samples taken during experiment 5. The excess-% ^{13}C is the difference between the fraction of ^{13}C of secondary organic carbon (SOC) and the blank (= sample holder) in percent ($f_{SOC} - f_b$) × 100). Particles were collected on the last 6 stages of the impactor. As expected from the size distribution, the stages 1 and 6 usually contained only little carbon mass (typically less than 20% of the stages 2−5) and the ^{13}C content was low. As most carbon was found on stages 2−5, their results were averaged. As is seen from Figure 3a these four stages showed a similar isotopic composition which also agreed well with the 2 simultaneous filter samples and the measurement from the electrostatic sampler. All measurements of the electrostatic sampler and average filter values are compared to the impactor (average of stages 2−5) data in Figure 3b. The good agreement among the three methods indicates that none of the methods suffers from major artifact problems. The relative errors of the measurements from the three methods were on average 15%.

Yield. The fraction of ^{13}C measured in the sample (f_s) was determined by an isotope mass-balance from the amount of

the carbon blank in the quartz filter or metal foil (C_b = blank), and the secondary organic carbon from α-pinene (SOC_p) and isoprene (SOC_i) according to

$$f_s \times C_s = f_b \times C_b + f_p \times SOC_p + f_i \times SOC_i \quad (1)$$

Since the ^{13}C fractions of SOC_p (f_p) and the blank (f_b) are almost equal we set $f_p = f_b$. For SOC of isoprene we used the isoprene ^{13}C fraction (f_i) of the labeled gaseous isoprene as measured by PTR-MS (Figure 1), which was around 0.8. We further assumed that the oxidation products of ^{13}C labeled isoprene partitioning into the aerosol retain the ^{13}C fraction of isoprene. Using the carbon mass balance

$$C_S = C_b + SOC_p + SOC_i \quad (2)$$

eq 1 can be rewritten as

$$f_s \times C_s = f_b \times C_s + (f_i - f_b) \times SOC_i \quad (3)$$

The mass fraction of secondary organic carbon from isoprene in the total organic carbon of the aerosol is then obtained from (see also Supporting Information)

$$\frac{SOC_i}{SOC_i + SOC_p} = \frac{f_s - f_b}{f_i - f_b} \times \frac{C_s}{C_s - C_b} = w_{SOC_i} \quad (4)$$

The yield of isoprene (Y_i) in the organic aerosol (ΔM_{OA}) is then given by

$$Y_i = \frac{\Delta M_{OA} \times w_{SOC_i} \times \gamma}{[\text{isoprene} - \text{reacted}]} \quad (5)$$

whereby the factor γ denotes the conversion of the amount of secondary organic carbon to organic mass for isoprene (OM_i) and α-pinene (OM_p) given by

$$\gamma = \frac{OM_i / SOC_i}{OM_p / SOC_p} \quad (6)$$

Both the ^{13}C fraction and the carbon content measured by the IRMS contribute to the uncertainty of the isoprene mass fraction (eq 4). The ^{13}C fraction was measured with an accuracy of $\pm 3 \times 10^{-6}$ while f_s is at least 3 times larger than $f_b = 0.010838$. Isotopic fractionation due to chemical reactions and partitioning can change f_s and f_i by only $\pm 5 \times 10^{-5}$. Therefore the first term in eq 4 has a very small uncertainty (~0.4%). The relative measurement error of the carbon content C_s and C_b is about 10% each. The error increases rapidly when the difference $C_s - C_b$ in the denominator of eq 4 becomes small. The relative error for the expression $C_s/(C_s - C_b)$ is calculated to be 7% at the lowest measured values ($C_s \approx 3 \times C_b$). The limit of detection of our measurement technique is determined by the difference $C_s - C_b$. Due to some trade-off of factors all methods reached similar limits of detection. Impactor sampling occurred at higher flow rates but the sample was distributed among four different stages. Sampling on filters and by electrostatic deposition was done at similar flow rates but the sampling efficiency in the latter was lower as stated above. On the other hand the carbon content in the sampling holder was higher for the filters compared to the tin foils used in the electrostatic sampler. More than 90% of the isoprene had reacted at the end of the experiment and the uncertainty of the term "isoprene-reacted" is below 10%. For the aerosol mass we estimate an uncertainty less than 20%. The factor γ has to be obtained from literature. Kleindienst et al. (*24*) and Aiken et al. (*25*) reported OM/OC ratios for aerosols from α-pinene (1.37 versus 1.67) and isoprene photooxidation (2.47 versus 1.75). On this basis the factor γ can range between 1.8 and 1.05.

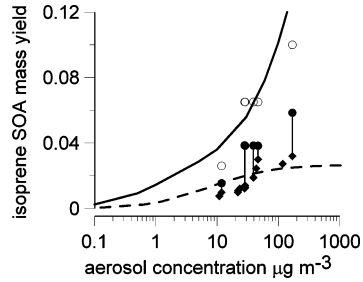

FIGURE 4. SOA yield of isoprene as function of total aerosol mass from this study (◆) using $\gamma = 1.05$ and compared to ref *13* (dashed line) and ref *14* (solid line). Final yields extrapolated to the point when all methacrolein would have reacted (see text) with $\gamma = 1.05$ (●) and $\gamma = 1.8$ (○). Model data of ref *13* were recalculated with an aerosol density of 1.25 g cm^{-3} as used in ref *14*.

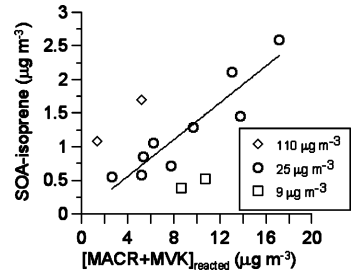

FIGURE 5. Dependence of the amount of SOA produced from isoprene and the sum of the reacted oxidation products methacrolein + methylvinylketone (MACR + MVK) at 9, 25, and 110 μg m^{-3} total organic aerosol mass concentration. The linear regression fit considers only data with 25 μg m^{-3} total organic aerosol mass concentration.

The large discrepancy of the OM/OC ratios for isoprene cannot be explained. The ratio may depend on the reaction conditions and time. Both studies were performed at similarly high precursor and aerosol concentrations.

The yield of isoprene as a function of SOA mass is presented in Figure 4 for the lower value of the factor γ. It increases from 0.01 at 10 μg m^{-3} to 0.03 at 100 μg m^{-3} of SOA. Figure 4 also depicts isoprene SOA yields used by Lane et al. (*13*) and Zhang et al. (*14*) for modeling the influence of isoprene on ambient regional SOA formation. Zhang et al. (*14*) applied the yields by Kroll et al. (*10*) obtained from the no-NO_x experiments, whereas Lane et al. (*13*) derived them from a set of published data from photooxidation experiments with NO_x. For $\gamma = 1.05$ our yield values compare well with the curve of Lane et al. whereas for $\gamma = 1.8$ they would be higher by a factor of 1.7 and fall somewhere between the two model studies.

Extent of Reaction. As pointed out by Chan et al. (*5*) the extent of the reaction is important in determining the yield of a precursor. Most of the SOA mass from isoprene stems from further oxidation of the first-generation oxidation product methacrolein (*26*). Under our experimental conditions with two precursors the second step of oxidation is slowed down and after 5−7 h often only a fraction of methacrolein had reacted away. From PTR-MS data we determined the fraction MACR + MVK reacted at the time of aerosol sampling. The correlation plot of m/z 75 (the fully labeled MVK + MACR) versus reacted isoprene is linear during the first 60−90 min of reaction before it starts to deviate from the straight line due to further reaction of MVK + MACR. The deviation from the extrapolated straight line yields the fraction of reacted MVK + MACR. As is seen in Figure 5 there is a good correlation between the amount of SOA from isoprene (= nominator in eq 5) and MVK + MACR reacted as was also observed by Ng et al. (*26*). The results are sorted

roughly according to the total organic aerosol mass, i.e., 9, 25, and 110 μg m^{-3}, which is determined by the initial α-pinene concentration. The three groups of data show the same trends. Extrapolating the values to zero should give as intercepts the amount of isoprene SOA from first-generation oxidation products. It appears that at the highest organic aerosol mass concentration a larger fraction of the isoprene SOA comes from first-generation oxidation products whereas at aerosol concentrations up to 25 μg m^{-3} no contribution of those is observed. Using this relation between the amount of isoprene SOA and MVK + MACR$_{reacted}$ we extrapolated the isoprene SOA yields to the point when all MVK + MACR would have reacted (final yields). These results are also shown in Figure 4 for $\gamma = 1.05$ (filled circles) and $\gamma = 1.8$ (open circles). For the higher SOA mass concentrations these final yields fall into the upper half between the two model curves (*13, 14*) while at 9 μg m^{-3} our values fall into the lower range. Due to the large spread of reported OM/OC ratios we are not able to better constrain the measured yields. Without this uncertainty the combined relative error of the yield from our measurements would be below 25%. This does not consider additional errors introduced by sample handling, which in some cases may be the cause of some extreme values we observed. More reliable OM/OC ratios are needed not only for this kind of analysis but also to better understand the aging of organic aerosols.

So far, SOA yields were only determined under conditions where the organic precursor produces all the aerosol mass. We have presented a method which decouples the SOA formation of the precursor from the main part of the absorbing organic aerosol mass. The results show that SOA yields from isoprene in an aerosol from α-pinene photooxidation are similar to those obtained by the "standard" way of measuring SOA yields. Due to sensitivity problems, i.e., mainly the carbon blank of the sample holders, we were not yet able to measure in the aerosol concentration range between 1 and 10 μg m^{-3}, which is frequently observed in rural and remote areas. By further reducing the blanks, the labeling technique described in this paper clearly has a high potential also for quantification of the SOA yield from isoprene at very low concentrations.

Acknowledgments

We thank R. Richter for construction of the plant chamber. This research was supported by the Swiss National Science Foundation as well as the EC projects EUROCHAMP, POLYSOA, and EUCAARI. H. Hellén acknowledges financial support from the Academy of Finland and Koneen Säätiö.

Supporting Information Available

Derivation of mathematical equations. This information is available free of charge via the Internet at http://pubs.acs.org.

Literature Cited

(1) Zhang, Q.; Jimenez, J. L.; Canagaratna, M. R.; Allan, J. D.; Coe, H.; Ulbrich, I.; Alfarra, M. R.; Takami, A.; Middlebrook, A. M.; Sun, Y. L.; Dzepina, K.; Dunlea, E.; Docherty, K.; DeCarlo, P. F.; Salcedo, D.; Onasch, T.; Jayne, J. T.; Miyoshi, T.; Shimono, A.; Hatakeyama, S.; Takegawa, N.; Kondo, Y.; Schneider, J.; Drewnick, F.; Borrmann, S.; Weimer, S.; Demerjian, K.; Williams, P.; Bower, K.; Bahreini, R.; Cottrell, L.; Griffin, R. J.; Rautiainen, J.; Sun, J. Y.; Zhang, Y. M.; Worsnop, D. R. Ubiquity and dominance of oxygenated species in organic aerosols in anthropogenically-influenced Northern Hemisphere midlatitudes. *Geophys. Res. Lett.* **2007**, *34*, L13801, doi: 10.1029/2007GL029979.

(2) Volkamer, R.; Jimenez, J. L.; San Martini, F.; Dzepina, K.; Zhang, Q.; Salcedo, D.; Molina, L. T.; Worsnop, D. R.; Molina, M. J. Secondary organic aerosol formation from anthropogenic air pollution: Rapid and higher than expected. *Geophys. Res. Lett.* **2006**, *33*, L17811, doi: 10.1029/2006GL026899.

(3) Hallquist, M.; Wenger, J. C.; Baltensperger, U.; Rudich, Y.; Simpson, D.; Claeys, M.; Dommen, J.; Donahue, N. M.; George, C.; Goldstein, A. H.; Hamilton, J. F.; Herrmann, H.; Hoffmann, T.; Iinuma, Y.; Jang, M.; Jenkin, M.; Jimenez, J. L.; Kiendler-Scharr, A.; Maenhaut, W.; McFiggans, G.; Mentel, T.; Monod, A.; Prevot, A. S. H.; Seinfeld, J. H.; Surratt, J. D.; Szmigielski, R.; Wildt, J. The formation, properties and impact of secondary organic aerosol: current and emerging issues. *Atmos. Chem. Phys. Discuss.* **2009**, *9*, 1–206.

(4) Kroll, J. H.; Chan, A. W. H.; Ng, N. L.; Flagan, R. C.; Seinfeld, J. H. Reactions of semivolatile organics and their effects on secondary organic aerosol formation. *Environ. Sci. Technol.* **2007**, *41*, 3545–3550.

(5) Chan, A. W. H.; Kroll, J. H.; Ng, N. L.; Seinfeld, J. H. Kinetic modeling of secondary organic aerosol formation: effects of particle- and gas-phase reactions of semivolatile products. *Atmos. Chem. Phys.* **2007**, *7*, 4135–4147.

(6) Kalberer, M.; Paulsen, D.; Sax, M.; Steinbacher, M.; Dommen, J.; Prevot, A. S. H.; Fisseha, R.; Weingartner, E.; Frankevich, V.; Zenobi, R.; Baltensperger, U. Identification of polymers as major components of atmospheric organic aerosols. *Science* **2004**, *303*, 1659–1662.

(7) Offenberg, J. H.; Lewis, C. W.; Lewandowski, M.; Jaoui, M.; Kleindienst, T. E.; Edney, E. O. Contributions of toluene and α-pinene to SOA formed in an irradiated toluene/α-pinene/NO_x/air mixture: Comparison of results using C-14 content and SOA organic tracer methods. *Environ. Sci. Technol.* **2007**, *41*, 3972–3976.

(8) Guenther, A.; Hewitt, C. N.; Erickson, D.; Fall, R.; Geron, C.; Graedel, T.; Harley, P.; Klinger, L.; Lerdau, M.; McKay, W. A.; Pierce, T.; Scholes, B.; Steinbrecher, R.; Tallamraju, R.; Taylor, J.; Zimmerman, P. A global model of natural volatile organic compound emissions. *J. Geophys. Res.* **1995**, *100*, 8873–8892.

(9) Kroll, J. H.; Ng, N. L.; Murphy, S. M.; Flagan, R. C.; Seinfeld, J. H. Secondary organic aerosol formation from isoprene photooxidation under high-NOx conditions. *Geophys. Res. Lett.* **2005**, *32*, L18808, doi: 10.1029/2005GL023637.

(10) Kroll, J. H.; Ng, N. L.; Murphy, S. M.; Flagan, R. C.; Seinfeld, J. H. Secondary organic aerosol formation from isoprene photooxidation. *Environ. Sci. Technol.* **2006**, *40*, 1869–1877.

(11) Dommen, J.; Metzger, A.; Duplissy, J.; Kalberer, M.; Alfarra, M. R.; Gascho, A.; Weingartner, E.; Prevot, A. S. H.; Verheggen, B.; Baltensperger, U. Laboratory observation of oligomers in the aerosol from isoprene/NOx photooxidation. *Geophys. Res. Lett.* **2006**, *33*, L13805, doi: 10.1029/2006GL26523.

(12) Henze, D. K.; Seinfeld, J. H. Global secondary organic aerosol from isoprene oxidation. *Geophys. Res. Lett.* **2006**, *33*, L09812, doi: 10.1029/2006GL025976.

(13) Lane, T. E.; Pandis, S. N. Predicted secondary organic aerosol concentrations from the oxidation of isoprene in the Eastern United States. *Environ. Sci. Technol.* **2007**, *41*, 3984–3990.

(14) Zhang, Y.; Huang, J. P.; Henze, D. K.; Seinfeld, J. H. Role of isoprene in secondary organic aerosol formation on a regional scale. *J. Geophys. Res.* **2007**, *112*, D20207, doi: 10.1029/2007JD008675.

(15) van Donkelaar, A.; Martin, R. V.; Park, R. J.; Heald, C. L.; Fu, T. M.; Liao, H.; Guenther, A. Model evidence for a significant source of secondary organic aerosol from isoprene. *Atmos. Environ.* **2007**, *41*, 1267–1274.

(16) Kesselmeier, J.; Staudt, M. Biogenic volatile organic compounds (VOC): an overview on emission, physiology and ecology. *J. Atmos. Chem.* **1999**, *33*, 23–88.

(17) Paulsen, D.; Dommen, J.; Kalberer, M.; Prévôt, A. S. H.; Richter, R.; Sax, M.; Steinbacher, M.; Weingartner, E.; Baltensperger, U. Secondary organic aerosol formation by irradiation of 1,3,5-trimethylbenzene-NO_x-H_2O in a new reaction chamber for atmospheric chemistry and physics. *Environ. Sci. Technol.* **2005**, *39*, 2668–2678.

(18) Taira, M.; Kanda, Y. Continuous generation system for low-concentration gaseous nitrous acid. *Anal. Chem.* **1990**, *62*, 630–633.

(19) Alfarra, M. R.; Paulsen, D.; Gysel, M.; Garforth, A. A.; Dommen, J.; Prevot, A. S. H.; Worsnop, D. R.; Baltensperger, U.; Coe, H. A mass spectrometric study of secondary organic aerosols formed from the photooxidation of anthropogenic and biogenic precursors in a reaction chamber. *Atmos. Chem. Phys.* **2006**, *6*, 5279–5293.

(20) Ng, N. L.; Chhabra, P. S.; Chan, A. W. H.; Surratt, J. D.; Kroll, J. H.; Kwan, A. J.; McCabe, D. C.; Wennberg, P. O.; Sorooshian, A.; Murphy, S. M.; Dalleska, N. F.; Flagan, R. C.; Seinfeld, J. H.

Effect of NOx level on secondary organic aerosol (SOA) formation from the photooxidation of terpenes. *Atmos. Chem. Phys.* **2007**, *7*, 5159–5174.
(21) Fierz, M.; Kaegi, R.; Burtscher, H. Theoretical and experimental evaluation of a portable electrostatic TEM sampler. *Aerosol Sci. Technol.* **2007**, *41*, 520–528.
(22) Maenhaut, W.; Hillamo, R.; Makela, T.; Jaffrezo, J. L.; Bergin, M. H.; Davidson, C. I. A new cascade impactor for aerosol sampling with subsequent PIXE analysis. *Nucl. Instrum. Methods Phys. Res.* **1996**, *109*, 482–487.
(23) Coplen, T. B.; Brand, W. A.; Gehre, M.; Groning, M.; Meijer, H. A. J.; Toman, B.; Verkouteren, R. M. New guidelines for delta C-13 measurements. *Anal. Chem.* **2006**, *78*, 2439–2441.
(24) Kleindienst, T. E.; Jaoui, M.; Lewandowski, M.; Offenberg, J. H.; Lewis, C. W.; Bhave, P. V.; Edney, E. O. Estimates of the contributions of biogenic and anthropogenic hydrocarbons to secondary organic aerosol at a southeastern US location. *Atmos. Environ.* **2007**, *41*, 8288–8300.
(25) Aiken, A. C.; Decarlo, P. F.; Kroll, J. H.; Worsnop, D. R.; Huffman, J. A.; Docherty, K. S.; Ulbrich, I. M.; Mohr, C.; Kimmel, J. R.; Sueper, D.; Sun, Y.; Zhang, Q.; Trimborn, A.; Northway, M.; Ziemann, P. J.; Canagaratna, M. R.; Onasch, T. B.; Alfarra, M. R.; Prevot, A. S. H.; Dommen, J.; Duplissy, J.; Metzger, A.; Baltensperger, U.; Jimenez, J. L. O/C and OM/OC ratios of primary, secondary, and ambient organic aerosols with high-resolution time-of-flight aerosol mass spectrometry. *Environ. Sci. Technol.* **2008**, *42*, 4478–4485.
(26) Ng, N. L.; Kroll, J. H.; Keywood, M. D.; Bahreini, R.; Varutbangkul, V.; Flagan, R. C.; Seinfeld, J. H.; Lee, A.; Goldstein, A. H. Contribution of first-versus second-generation products to secondary organic aerosols formed in the oxidation of biogenic hydrocarbons. *Environ. Sci. Technol.* **2006**, *40*, 2283–2297.

ES9006959